Title
Characteristics of human-climate feedbacks differ at different radiative forcing levels

Authors
Calvin, Katherine
Bond-Lamberty, Ben
Jones, Andrew
et al.

Publication Date
2019-09-01

DOI
10.1016/j.gloplacha.2019.06.003

Peer reviewed

Characteristics of human-climate feedbacks differ at different radiative forcing levels

Katherine Calvin[1], Ben Bond-Lamberty[1], Andrew Jones[2], Xiaoying Shi[3], Alan Di Vittorio[2], Peter Thornton[3]

Affiliations:

[1] Joint Global Change Research Institute, Pacific Northwest National Laboratory, College Park, MD USA

[2] Lawrence Berkeley National Laboratory, Berkeley, CA USA

[3] Environmental Sciences Division and Climate Change Science Institute, Oak Ridge National Laboratory, Oak Ridge, TN USA

Corresponding author: Katherine Calvin (katherine.calvin@pnnl.gov)

Abstract: *The human and Earth systems are intricately linked: climate influences agricultural production, renewable energy potential, and water availability, for example, while anthropogenic emissions from industry and land use change alter temperature and precipitation. Such feedbacks have the potential to significantly alter future climate change. These feedbacks may also exert significant changes on 21st-century energy, agriculture, land use and carbon cycle projections, but little is known about their possible magnitudes, or about regional and sector dynamics under different forcing scenarios. Here we use an integrated Earth System Model (ESM) featuring bidirectional information exchange between an economically-oriented integrated assessment model and the ESM to examine how human-natural feedbacks operate under high and medium radiative forcing (RF) scenarios. Specifically, we examine the effect of changing land productivity on human systems, and the effect of changing land use/land cover and CO_2 emissions on the Earth system. We find that the effect of coupling differs across radiative forcing levels and across regions, due to differences in the climate signal, human responses to those signals, and regional characteristics. In particular, we find reductions in cropland area due to feedbacks in both the medium and high RF scenarios. In the medium RF scenario, these reductions result in increased area for bioenergy and afforestation and reduced energy system CO_2 emissions, as the carbon price in this scenario incentivizes low carbon energy sources and terrestrial carbon storage; these incentives are absent in the high RF scenario. These differences are key to understanding the possible future evolution pathways of the integrated Earth system in response to 21st century climate change. Additional models and hypothesis testing are needed to determine exactly when and how bidirectional feedbacks between human and Earth systems should be considered in future assessments.*

1 Introduction

Changes in energy and agricultural production and consumption affect anthropogenic greenhouse gas emissions, land use, and land cover (Berndes

et al. 2003; Houghton et al. 2012) with implications for temperature, precipitation, and other aspects of the climate system, resulting in changes in energy demand and production (Arent et al. 2014). Likewise, climate-driven changes to net primary production (NPP) and the carbon cycle affect terrestrial carbon storage, forest productivity, and CO_2 concentrations (Piao et al. 2009), while increases (decreases) in agricultural productivity may lead to reductions (increases) in cropland area, as more (less) food and fiber can be produced the same amount of land (Nelson et al. 2014).

One-way coupling studies have estimated the effects of human activities on climate. For example, Collins et al. (2013) quantifies the effect of different emissions and concentrations scenario on climate, with 2100 global mean temperature rise ranging from 0.3℃ to 4.8℃ depending on the climate model and scenario scales. Brovkin et al. (2013) and Hallgren et al. (2013) show that changes in land use have a negligible effect on global climate, but can have an effect at local scales. Jones et al. (2013), however, find significant effects on global temperature from changes in land use and land cover. Other studies have focused on quantifying the effects of climate on human activities. For example, Nelson et al. (2014) finds that changes in climate can result in large changes in cropland extent. Reilly et al. (2007) find that increases in greenhouse gases can increase crop yields, but the inclusion of ozone pollution results in reduced yield.

Bidirectional feedbacks from climate to energy and land, however, have largely been excluded from previous literature: the Representative Concentration Pathways (RCPs) (Moss et al. 2010; van Vuuren et al. 2011) project future emissions and land use, land-cover change (LULCC) assuming the climate is not changing, while estimates of the influence of climate on human systems (e.g., the Agricultural Model Intercomparison and Improvement Project, AgMIP (Nelson et al. 2014; Rosenzweig et al. 2014)) assume that the changes induced do not feed back to the climate. Ignoring these feedbacks may bias estimates of climate change and estimates of climate impacts (Hallegatte and K. J. Mach 2016; Motesharrei et al. 2016; Palmer and Smith 2014), but the unknown magnitude of these feedbacks, and the complexity of modeling these interactions, has led to limited analyses of bidirectional human—Earth system feedbacks.

There are three notable exceptions (see also (Calvin and Bond-Lamberty 2018)). First, Voldoire et al. (2007) coupled the IMAGE Integrated Assessment Model (IAM) with the CNRM-CM3 atmosphere-ocean General Circulation Model (GCM), and found that non-climatic factors dominated over climatic ones in determining land-use patterns in an SRES A2 scenario. Second, the BNU-HESM model coupled the BNU Earth System Model (ESM) to the DICE IAM, exchanging CO_2 emissions and temperature every 10 years (Yang et al. 2015). The authors found that including a human component improved prediction of temperature, but degraded prediction of CO_2 concentrations in a historical period. Finally, the integrated Earth System Model (iESM; https://github.com/E3SM-Project/iESM; Collins et al., 2015)

includes a bidirectional information exchange between the IAM and the ESM, including land use, land cover, CO_2 emissions, and terrestrial productivity (see Section 2). Thornton et al. (2017) used the iESM to quantify the effects of human—Earth system feedbacks via the terrestrial system in an RCP4.5. In that analysis, changes in climate and CO_2 increased the productivity of land, resulting in the abandonment of cropland and expansion of forest cover. Little is known, however, about how generalizable these results may be under different climatic and policy conditions.

Here we use the modeling framework documented in Collins et al. (2015) and used in Thornton et al. (2017). This modeling framework links human and Earth systems through terrestrial feedbacks, with changes in ecosystem productivity in the Earth system altering human dynamics and changes in land use, land cover and CO_2 emissions in the human system altering Earth system dynamics. We use this framework to examine a key sensitivity arising from the baseline emissions scenario, focusing in particular on the regional characteristics of the coupled human—Earth system in a high-emissions scenario (RCP8.5). The significance of examining a higher emissions scenario is two-fold. First, higher emissions lead to a larger climate change signal. At the same time, energy and agricultural systems are less constrained by climate policy in a higher emissions scenario, altering the magnitude and characteristics of human responses to climate feedbacks. Section 2 describes the modeling framework and scenarios used in this study. Section 3 presents results related to effects on the human system (Section 3.1), implications for the Earth system (Section 3.2), and differences between the RCP4.5 and RCP8.5 (Section 3.3). Section 4 provides a discussion of the findings and their implications for future climate prediction studies.

2 Methods

2.1 The iESM

The iESM (Collins et al. 2015) is a bidirectional coupling between an IAM (the Global Change Assessment Model, GCAM) and an ESM (the Community Earth System Model, CESM). As a result, the model can capture the effects of climate on human systems, as well as the effects of changes in human systems on climate. GCAM is a global integrated assessment model, linking together representations of the economy, energy system, and agriculture and land use system (Wise et al. 2014). The model computes supply, demand, and price for a variety of energy and agricultural commodities. GCAM calculates land use and land cover change associated with producing those agricultural commodities, as well as CO_2 emissions from the energy system.[1] Within each GCAM land region (151 global regions), land is allocated across a variety of uses based on expected profit, which is a function of commodity price, yield, and the cost of production. Profits will

[1] GCAM also calculates non-CO_2 emissions. However, the iESM uses prescribed non-CO_2 emissions from the RCP4.5 scenario, rather than the emissions calculated endogenously by GCAM.

change as a result of changes in climate and CO_2, through both direct effects on yield and indirect effects via changes in price. The land system is linked to the energy system primarily through bioenergy, which is produced by the land and consumed by the energy system. Changes in land profitability, therefore, have implications for energy production, use and associated emissions. The iESM uses version 3.0 of GCAM.

CESM (Hurrell et al. 2013) couples representations of the atmosphere, ocean, and land to produce simulations of Earth's climate in the past, present, and future. The CESM system comprises the Parallel Ocean Program, version 2 (POP), the Community Land Model, version 4.0 (CLM 4.0), the Los Alamos sea-ice model (CICE), the Community Atmosphere Model, version 5 (CAM), and the Community Ice Sheet Model (CISM). CESM is run with active biogeochemistry in the atmosphere, ocean, and land (Long et al. 2013). CO_2 concentrations are calculated by CAM based on energy system emissions (calculated by GCAM), terrestrial carbon flux (calculated by CLM), and ocean carbon uptake (calculated by POP). CLM includes the effects of N stress on carbon uptake (Thornton et al. 2009). CESM has lower terrestrial carbon uptake than many other ESMs; however, ocean carbon uptake is close to the mean across ESMs (Friedlingstein et al. 2014).

In the iESM, information is passed from GCAM to CESM and from CESM to GCAM every five years (see Figure 1 and Table 1). The information exchange from GCAM to CESM occurs in all simulations. In particular, gridded land use and energy system CO_2 emissions are passed from GCAM to CESM. Land use and emissions are downscaled from GCAM’s regional representation to a grid following the protocols developed for the RCPs (Thomson et al. 2011). Terrestrial CO_2 fluxes are computed within the land component of CESM, and change over time as the result of land use change (including deforestation), changes in climate, and CO_2 fertilization. For non-CO_2 emissions, we use the original RCP concentrations, and not those generated by GCAM. That is, non-CO_2 emissions evolve in time and vary across RCP, but are not altered by climate feedbacks. In the Coupled simulations in this paper, net primary productivity (NPP) and heterotrophic respiration (HR) are passed from CESM to GCAM, and used to adjust the agricultural yield and terrestrial carbon density in GCAM to reflect changes in climate and CO_2 fertilization (Bond-Lamberty et al. 2014). NPP and HR are averaged across time and GCAM region. In the Uncoupled simulations, no information is passed back to GCAM; instead, agricultural yields exclude the influence of changes in climate or CO_2 fertilization. For agricultural yields, GCAM includes 12 crop categories, representing all agricultural commodities reported by the FAO. CESM has a single crop, but the effect of climate on crops will vary across the 12 GCAM crop categories because different crops are grown in different regions and thus we aggregate different climate signals for each crop category.

This coupling happens in an online mode; that is, information is exchanged in code. The coupling time step is five years and information is lagged between

those coupling steps. The iESM model is available at: https://github.com/E3SM-Project/iESM.

Figure 1: iESM Coupling Diagram. Diagram shows the exchange of information between GCAM (left) and CESM (right). Arrows indicate the flow of information between components, with the text label identifying the type of information exchanged. The arrow labeled "climate, productivity, etc." is only included in the Coupled simulations. All other information exchanges occur in all simulations.

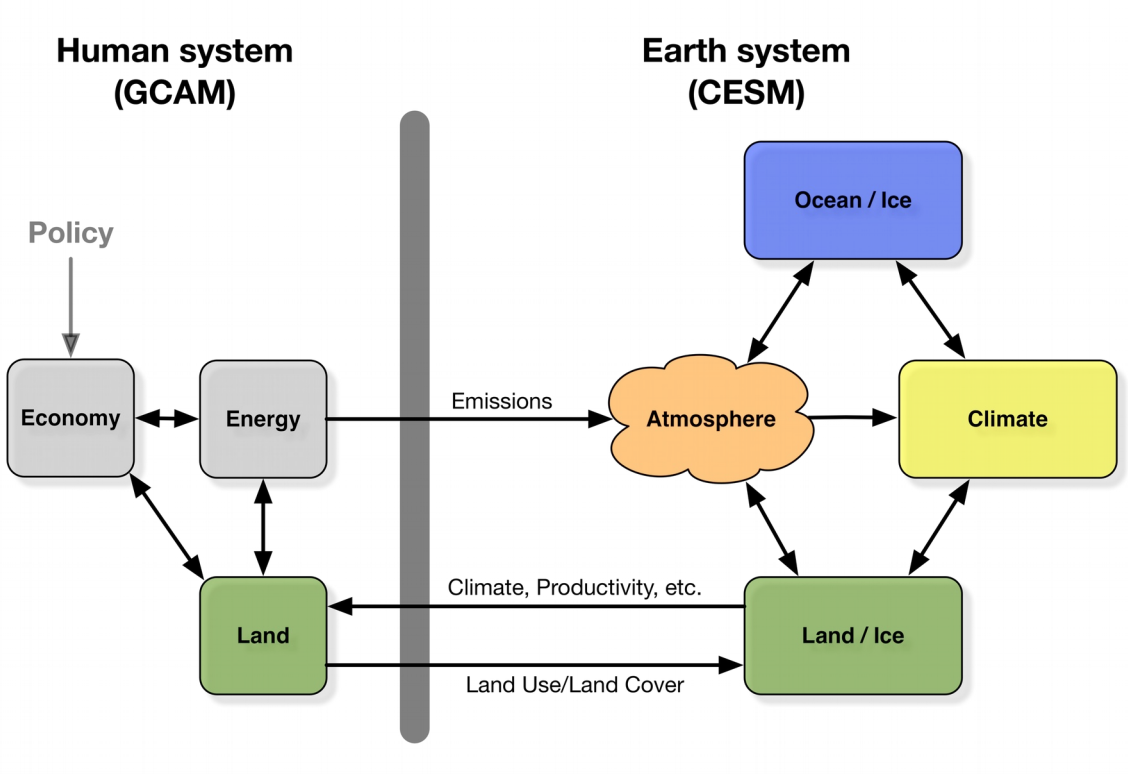

Table 1: Variables that are exchanged dynamically in the iESM, including the transformations required in the data exchange. Note that the final two columns only include examples of the direct and indirect effects of this information exchange. There are further effects that will occur in each model.

Direction of Exchange	Variable from source model	Transformation required	Variable in destination model	Examples of variables directly affected in destination model	Examples of secondary effects
GCAM	Land use	Downscaled	Land use	Carbon	Temperat

to CESM	and land cover	from 151 regions and 27 land types to a 1º grid and 15 PFTs	and land cover	storage, albedo, evapotranspiration	ure, precipitation
GCAM to CESM	Fossil fuel and industrial CO_2 emissions	Downscaled from 14 regions to a 1º grid	Fossil fuel and industrial CO_2 emissions	CO_2 concentration	Temperature
CESM to GCAM	Net primary productivity	Upscaled from 1º grid and 15 PFTs to 151 regions and 27 land types; indexed to calculate change from base year	Crop yield	Profit rates by land type, crop production, bioenergy production	Land use and land cover, crop prices, CO_2 emissions
CESM to GCAM	Net primary productivity (NPP)	Upscaled from 1º grid and 15 PFTs to 151 regions and 27 land types; indexed to calculate change from base year	Vegetation carbon density	Profit rates by land type[a]	Land use and land cover[a]
CESM to GCAM	Heterotrophic respiration	Combined with NPP, upscaled from 1º grid and 15 PFTs to 151 regions and x land types; indexed to calculate	Soil carbon density	Profit rates by land type[a]	Land use and land cover[a]

		change from base year			

[a] Note that changes in carbon density only affect profit rates, and consequently land use and land cover, when carbon prices are applied.

2.2 Scenarios

The scenarios described in this paper vary across two dimensions: radiative forcing and feedbacks. We include scenarios with and without feedbacks to the human system, where feedbacks are communicated as changes in productivity of the terrestrial system. We also consider two different radiative forcing levels: medium and high. The medium forcing level reaches 4.5 W/m^2 in 2100 in the scenario without feedbacks to the human system, and the high forcing level reaches 8.5 W/m^2 in 2100 without feedbacks. The forcing level in scenarios with feedbacks may differ from those levels; for ease of communication, we refer to the scenarios with and without feedbacks by their no feedbacks forcing level. Table 2 summarizes these scenarios and establishes a naming convention used in the paper.

Table 2: iESM Simulations Used in this Paper. Columns indicate 2100 radiative forcing level in the scenario without feedbacks; rows indicate whether feedbacks to the human system are included. Cell values are the names of the simulations used in the remainder of the paper. While the forcing level may differ between the coupled and uncoupled simulations, we use the same radiative forcing label for both.

		2100 Radiative Forcing	
		4.5 W/m^2	8.5 W/m^2
Feedbacks to the Human System	Excluded	Uncoupled45	Uncoupled85
	Included	Coupled45	Coupled85

2.2.1 The 4.5 W/m^2 Scenarios

The Coupled45 and Uncoupled45 scenarios stabilize radiative forcing at 4.5 W/m^2 in 2100 through the imposition of a carbon price. These scenarios are updated versions of the RCP4.5 (Thomson et al. 2011). They differ from the scenarios described in Thornton et al. (2017) in that these simulations exchange information on fossil fuel CO_2 emissions directly from GCAM to CESM.

2.2.2 The 8.5 W/m^2 Scenarios

The Coupled85 and Uncoupled85 scenarios use the GCAM integrated assessment model to replicate the RCP8.5, originally produced by the MESSAGE model (Riahi et al. 2011). In particular, we use population and GDP from the RCP8.5 scenario. All other technological assumptions are based on those used in the GCAM3.0 (Clarke et al. 2007; Wise et al. 2014). The RCP8.5 scenario, like the original, does not include a carbon price or any other climate policy. The resulting scenario has comparable energy system CO_2 emissions and land cover to the original RCP8.5 (SI Figure 1). Note that MESSAGE includes a woody bioenergy crop and GCAM includes a grassy bioenergy crop. These differences result in differences in total cropland area (GCAM is higher due to the inclusion of bioenergy), but non-energy crop area is virtually identical between the two scenarios.

2.2.3 Scenario Differences

The difference between the Uncoupled45 and Uncoupled85 used in this paper is due to differences in both socioeconomics (income and population) and climate policy. To isolate these effects, we supplement the iESM simulations with two additional standalone GCAM simulations, Socio45_noClimatePolicy and Socio85_withClimatePolicy (see Table 3). These additional simulations include one case with the Uncoupled85 socioeconomics and the Uncoupled45 climate policy and one case with the Uncoupled45 socioeconomics and the Uncoupled85 climate policy (i.e., no policy). As these cases were run in a standalone version of GCAM, they exclude climate feedbacks and can only be compared to the Uncoupled iESM cases.

Table 3: Simulations used to decompose the effects of human-Earth system feedbacks, socioeconomics, and climate policy. Note that the four scenarios are equivalent to those introduced in Table 2; only two additional scenarios are introduced for this decomposition.

Socioeconomics	Climate Policy	Feedbacks	Scenario Name
RCP4.5	Yes	No	Uncoupled45
RCP4.5	Yes	Yes	Coupled45
RCP4.5	No	No	Socio45_noClimatePolicy
RCP8.5	No	No	Uncoupled85
RCP8.5	No	Yes	Coupled85
RCP8.5	Yes	No	Socio85_withClimatePolicy

3 Results

3.1 The effect of human-Earth system feedbacks on the human system

The RCPs (Moss et al. 2010; van Vuuren et al. 2011) were designed around specific changes in radiative forcing, determined by various assumptions affecting energy, emissions, and land use, resulting in increases in CO_2 concentrations, increases in temperature, and changes in precipitation patterns (SI Figure 2). In iESM (like other ESMs, e.g., (Arora and Boer 2014; Shao et al. 2013), these changes can increase plant productivity: annual global NPP at the end of the 21st century is ~9 Pg C (~18%) higher than today in an 8.5 W m^{-2} simulation and ~7 Pg C (15%) higher in a 4.5 W m^{-2} simulation. Those global changes are seen in most, but not all, parts of the world (Figure 2).

Figure 2: Above ground scalar for forest (top) and crops (bottom) in 2071-2090. Scalar is the change in NPP over time. A value of one indicates no change in NPP due to changes in climate. Values above one (green colors) indicate increases; values less than one indicate decreases. CLM calculates NPP at the grid cell; these are averaged to GCAM regions for this plot. Changes are due to changes in climate and CO_2 fertilization.

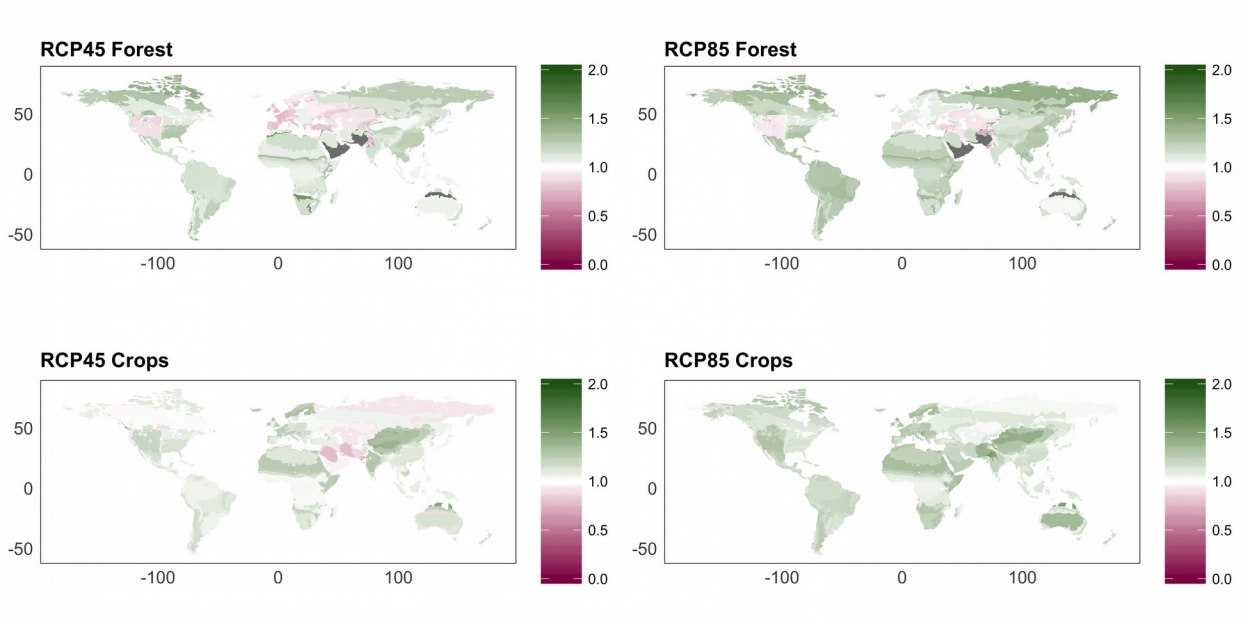

Increases in productivity in both scenarios alter agricultural yields. In response, crop prices and thus cropland profit rates decline, resulting in less cropland area when feedbacks are included (Figure 3). Crop prices in 2090 decline by 15-16% for corn, 15-17% for oil crops, and 16-18% for wheat. The resulting decline in cropland area, relative to the Uncoupled simulations in 2090, is significant: ~1 million km^2 (7%) in the Coupled45 and ~2 million km^2 (10%) in the Coupled85. These declines nearly balance the increases in productivity, resulting in only small increases in crop production due to

human—climate feedbacks (~1% in 2090 in both the Coupled45 and Coupled85). This balancing is expected given the relatively low price elasticity of agricultural demand. However, these declines in cropland area do result in increases in non-commercial forestland by 1.3 million km^2 (~3%) in the Coupled45 and 1.8 million km^2 (~6%) in the Coupled85.

Figure 3: Change in global land cover over time due to coupling in million km^2. GCAM calculates changes in land cover by land type at the regional scale as a result of changes in climate and CO_2 from CESM. Land types are aggregated to seven categories for purposes of plotting. A full list of land types and their mapping to these categories is provided in the SM.

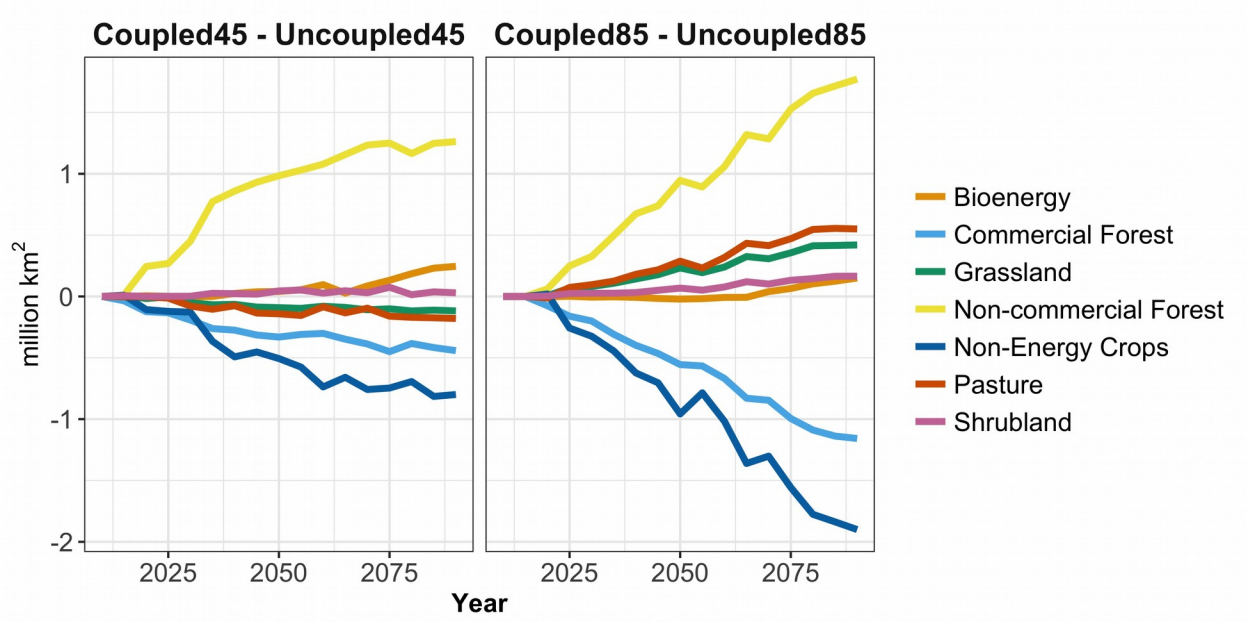

At the regional level, the dynamics are more complex: there are 29 subregions where cropland expands in the RCP4.5 and 12 regions in the RCP8.5; in 36 of these 41 subregions, yields increase (Figure 4; SI Figure 3). This effect is because land owners maximize profit; all else equal, an increase in yield results in an increase in profit and an increase in land area. However, prices adjust to ensure global supply and demand equilibrate; as a result, regional yield increases do not always equate to regional cropland increases. For example, we see modest increases in cropland area in northern Africa and India in Coupled45 (Figure 4). These correspond directly to the increases in NPP shown in Figure 2. The effect of these changes on forest and other land cover types differs somewhat between the RCP4.5 and RCP8.5 (see Section 3.3), but there is a strong relationship between declines in cropland area in a region and increases in forest cover.

Figure 4: Change in forest (top) and cropland (bottom) area due to coupling for 2071-2090 in million km². Positive numbers (green colors) indicate increases in area and negative numbers (pink colors) indicate decreases in area, as a result of changes in NPP and HR. Forest includes both commercial and non-commercial forests. Cropland includes all food, feed, and fiber crops, but excludes dedicated bioenergy crops.

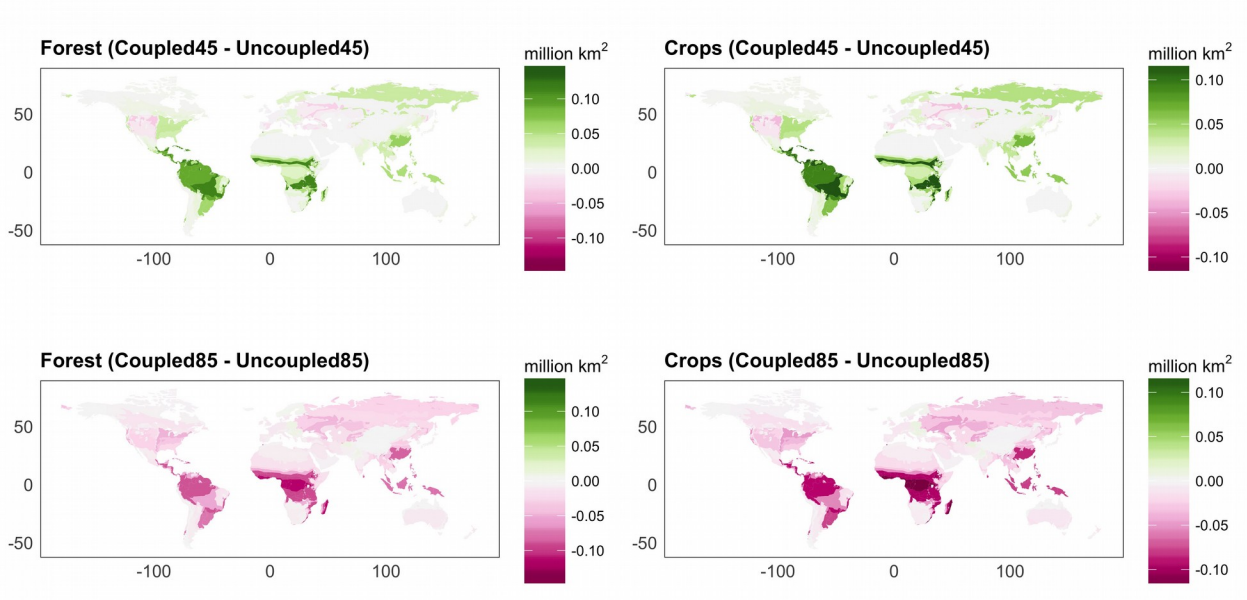

The reallocation of land in the Coupled45 also increases the area of bioenergy crops by 0.25 million km² and its production by 33 EJ yr^{-1} (~18%) in 2090 as compared to the Uncoupled45. The Coupled85, however, has an increase of only 0.15 million km² (9 EJ yr^{-1}, +5%) over the Uncoupled85. The increased bioenergy production in both scenarios shifts energy production away from fossil fuel technologies, resulting in decreased consumption of these fuels. Total fossil fuel consumption in 2100 declines by 13 EJ yr^{-1} (~2.5%) in the Coupled45 and by 1.5 EJ yr^{-1} (~0.5%) in the Coupled85, compared to the Uncoupled simulations. The decreased consumption of fossil fuels also decreases energy system CO_2 emissions (Figure 5). The effect is small in the Coupled85 (~1% of total emissions), but significant in Coupled45, with emissions decreasing by ~700 MtC yr^{-1} in 2090 (~15% of total emissions). The smaller effect on bioenergy and emissions in the Coupled85, despite higher productivity gains, is due to the underlying scenario assumptions: only the Coupled45 and Uncoupled45 simulations include a carbon price as a means of reducing emissions, incentivizing low carbon energy technologies, as described in Section 3.3. This incentive results in a larger increase in bioenergy consumption and larger decrease in energy system emissions due to feedbacks in the Coupled45. Additionally, the Uncoupled45 has lower emissions than the Uncoupled85 due to this

carbon price; as a result, the same absolute reduction in emissions leads to a larger reduction in percentage terms in the Coupled45 than the Coupled85.

Figure 5: Percentage change in energy system CO_2 emissions in 2071-2090 due to coupling. Positive values (red colors) indicate increases in energy system emissions; negative values (blue colors) indicate decreases.

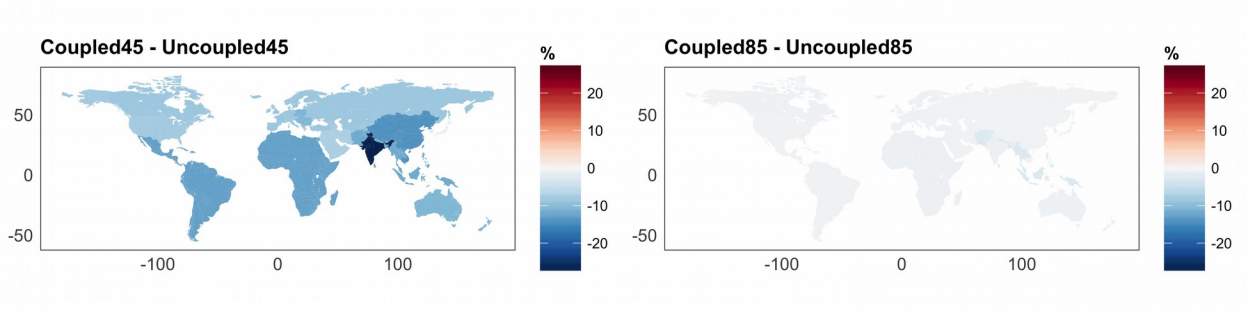

3.2 The effect of human-Earth system feedbacks on the Earth system

The reallocation of land in the Coupled simulations has significant implications for terrestrial carbon sequestration, with more carbon stored in the terrestrial system and less in the atmosphere (SI Figure 4). In both the Coupled45 and Coupled85, the reduction in carbon in the atmosphere is ~10 Pg C by 2090 with a corresponding reduction in CO_2 concentrations of ~5 ppmv in 2090 in both the Coupled45 and the Coupled85.

Regions with increases in forest cover (Figure 4) tend to have increases in carbon storage (Figure 6), although this is not universally true. For example, the Amazon basin shows declines in carbon storage in the Coupled85 despite increases in noncommercial forest cover. These declines are due to the land use and land cover transition and in part to changes in NPP. While noncommercial forest increases significantly, some of that increase is at the expense of commercial forest, resulting in only modest increases in total forest area due to coupling (SI Figure 5). While the region-wide average NPP increases (see Figure 2) driving the increase in total forest area, NPP declines in individual grid cells over large parts of the Amazon (SI Figure 6). This decline is likely due to increased evaporative demand (driven by higher air temperatures) and drought stresses in the RCP8.5 scenarios that result in increased forest mortality and thus carbon loss (Anderegg et al. 2015; Holm et al. 2014).

Figure 6: Change in terrestrial carbon storage in 2071-2090 due to coupling, in gC/m^2/yr. Positive values (green colors) indicate increases in terrestrial carbon; negative values indicate decreases. Changes in carbon are due to both changes in land use/land cover and changes in carbon density due to climate and CO_2 fertilization.

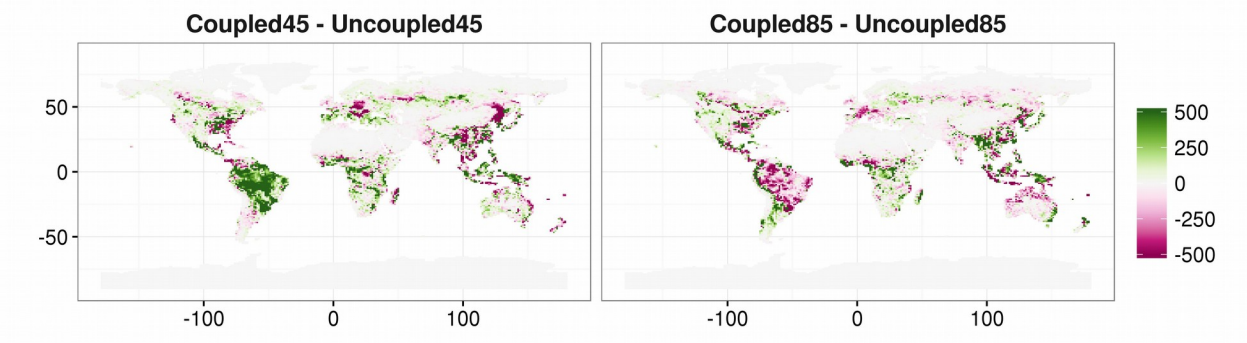

Such small changes in energy system emissions (Figure 5) and terrestrial carbon storage (Figure 6) lead to only small changes in atmospheric carbon and a seemingly negligible change in trends and variability of global mean temperature (GMT; SI Figure 7). However, local temperature differences can be as much as ±1℃ (Figure 7). The changes in local temperature are influenced by local land use change; thus, we see consistent patterns in Figure 4 and Figure 7. For example, the Coupled85 shows increases in forest cover and more warming in the Siberia as compared to the Uncoupled85.

Figure 7: Average change in temperature in 2071-2090 due to coupling in ℃. Positive values (red colors) indicate increases in temperature due to human feedbacks; negative values (blue colors) indicate decreases. Stippling indicates significant changes at the 95% confidence level using a t-test.

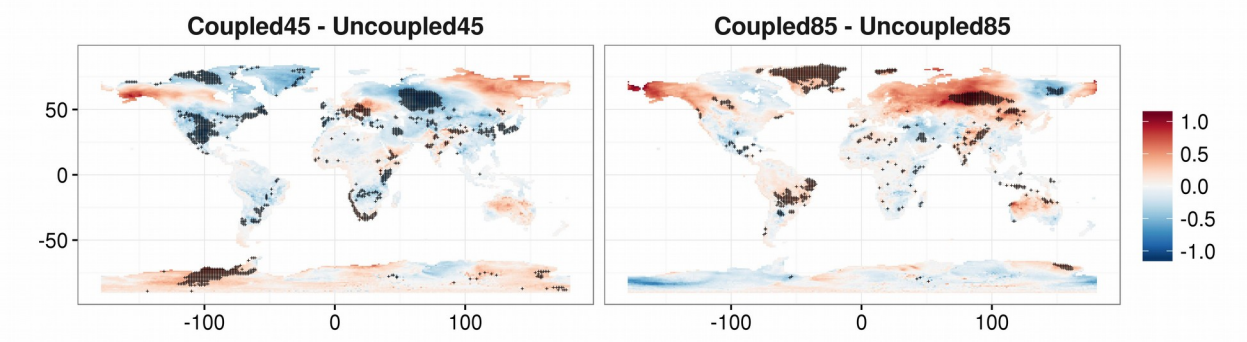

3.3 Differences between the 45 and 85

It is important to note that the Uncoupled simulations differ significantly between the 4.5 Wm^{-2} and 8.5 Wm^{-2}, with the 4.5 Wm^{-2} including significant afforestation and the 8.5 Wm^{-2} including significant increases in CO_2 emissions (SI Figure 8). These differences are due to differences in

population, income, and climate policy. The Uncoupled85 has a larger population and higher total GDP than the Uncoupled45, both factors that lead to increases in agricultural demand and cropland area. The Uncoupled45 includes an explicit value on carbon, resulting in reductions in emissions and increases in forest cover.

To understand the relative land cover and emissions implications of human-Earth sytem feedbacks compared to socioeconomic and climate policy assumptions in the scenarios, we supplement our analysis with additional uncoupled GCAM simulations. These simulations systematically change socioeconomics and climate policy to isolate the effects of each. In particular, we examine the following additional uncoupled scenarios: 1) RCP4.5 socioeconomics without climate policy, and 2) RCP8.5 socioeconomics with climate policy (see also Table 3).

Climate policy has the most significant effect on emissions and land cover (Figure **8**). Emissions decline by ~20 GtC/yr in 2090 with the imposition of a climate policy (17 GtC/yr under RCP4.5 socioeconomics and 22 GtC/yr under RCP8.5 socioeconomics). This effect is much larger than the effect of changing socioeconomic conditions, which result in a 1.5 GtC/yr (with climate policy) to 5.5 GtC/yr (without climate policy) reduction in emissions when moving from the high population (RCP8.5) to low population (RCP4.5) cases. In contrast, human-Earth system feedbacks lead to a decrease in emissions of 0.3 (Coupled85) to 0.7 GtC/yr (Coupled45).

Figure 8: Decomposing the Effect of Socioeconomics, Climate Policy, and Human-Earth System Feedbacks on CO_2 (left), Cropland (middle), and Non-commercial Forest (right). Figures show differences due to socioeconomics (top), climate policy (middle), and human-Earth system feedbacks (bottom). Note that the control changes to isolate the appropriate factor; the legend indicates the scenarios that are differenced for each calculation. In the top row, positive values indicate an increase with RCP4.5 socioeconomics (as compared to RCP8.5). In the middle row, positive values indicate an increase with climate policy. In the bottom row, positive values indicate an increase with human-Earth system feedbacks.

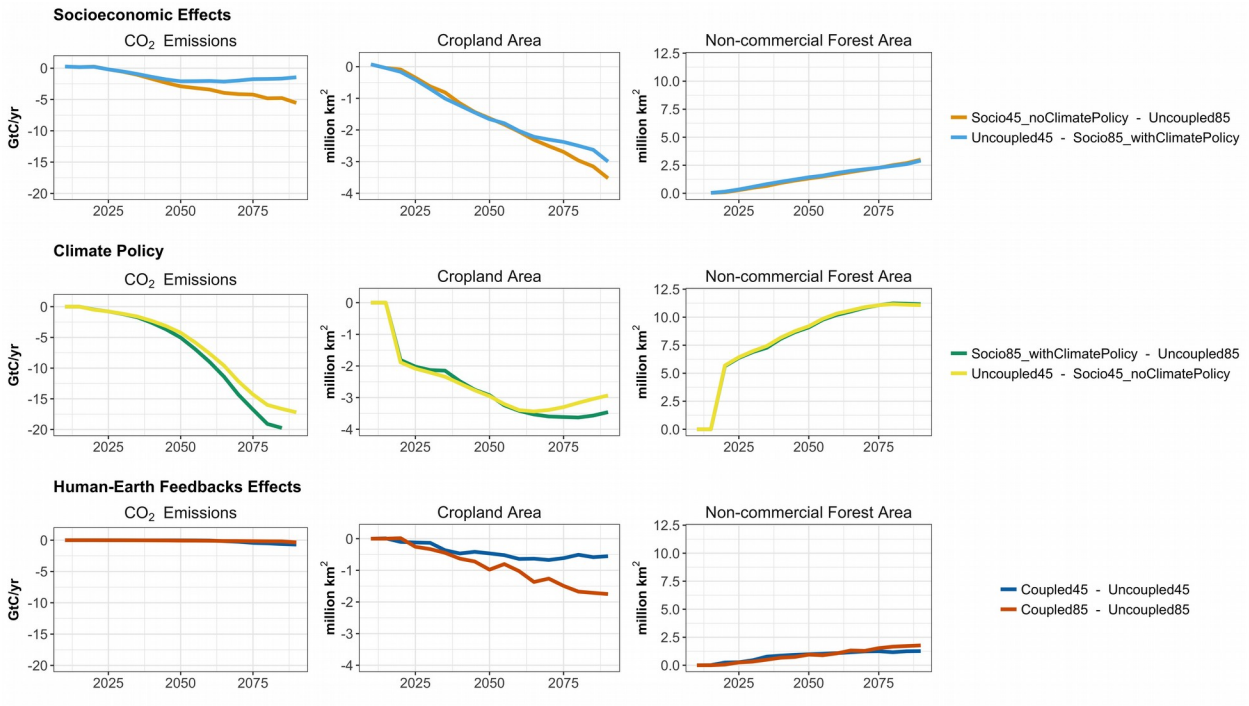

Forest cover increases immediately when the climate policy begins and continues throughout the century (~10 million km^2 increase in 2090 with climate policy); this increase is significantly larger than the small increase (~3 million km^2 in 2090) associated with lower population and GDP. Human-Earth system feedbacks result in increases of forest cover of approximately 1 million km^2 in 2090. In response to increases in forest cover in scenarios with climate policy, cropland declines by approximately 3 million km^2 in 2090. Declines in population and GDP also result in ~3 million km^2 decreases in cropland, while feedbacks lead to a 1-2 million km^2 decrease in cropland area in 2090. That is, the effect of feedbacks is roughly half the size of the effect of changing GDP and population in most cases.

Differences in the underlying dynamics of the scenarios have implications for the response to climate feedbacks, particularly with respect to land use/land cover change. In both the 4.5 Wm^{-2} and the 8.5 Wm^{-2}, less cropland is needed when feedbacks are included due to increases in productivity.

However, the primary land type that benefits in response to less cropland differs by region and scenario (Figure 9, SI Figure 5). In the 4.5 Wm^{-2}, the climate policy is applied to the terrestrial system, incentivizing higher carbon land types and causing an overall decline in cropland that is enhanced when feedbacks are included. In the 8.5 Wm^{-2}, such incentives do not exist and cropland expands, but at a slower rate when feedbacks are included. As a result, the dominant expanding land type due to the inclusion of feedbacks depends on the cropland trajectory and the regional land type distribution. For example, enhanced crop abandonment leads primarily to forest increases throughout South America in Coupled45, while in Coupled85 reduced cropland expansion primarily retains pasture, grass, and shrub in the southern part of the continent.

Figure 9: Dominant expanding land type in 2071-2090 when feedbacks induce less demand for cropland. That is, the land type that increases the most in response to reductions in cropland area for each region. Missing regions (i.e., white colors) have increases in cropland area.

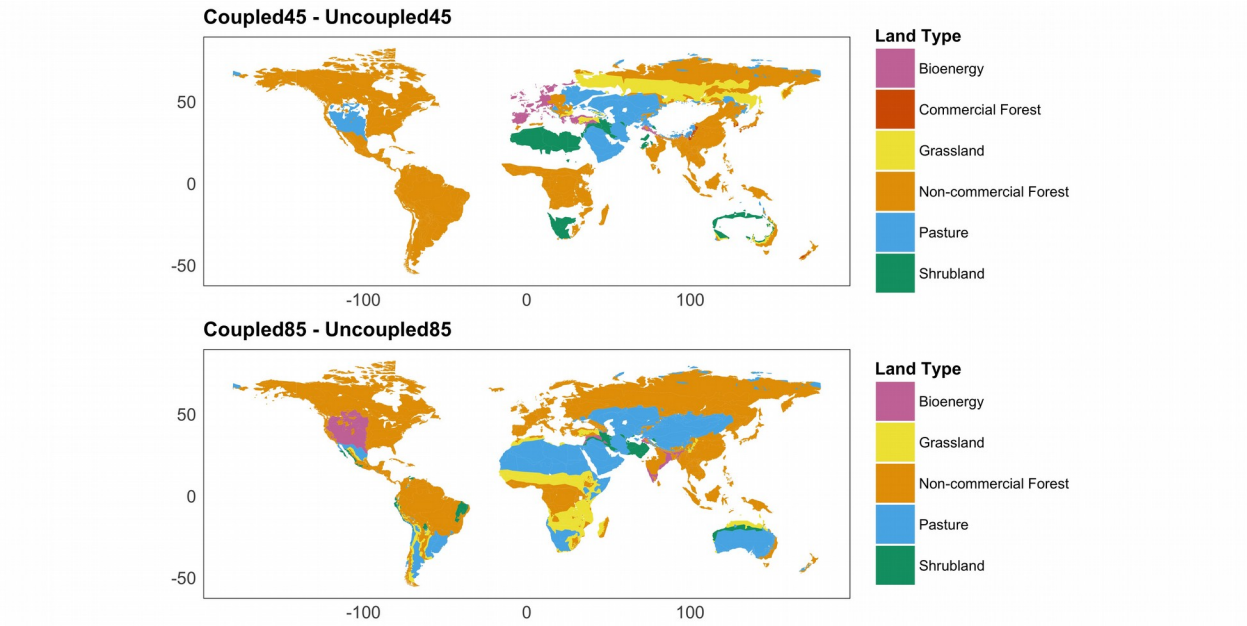

4 Discussion and Conclusions

We find that the effects of human—Earth system feedbacks differ at different radiative forcing levels. These differences are due in part to differences in the climate signal, resulting in different productivity changes. However, the response of human systems also varies because of differences in socioeconomic and climate policy assumptions, complicating any comparison of a single factor shared by the two scenarios. In particular, the RCP45 incentivizes economic actors to retain and expand (via cropland abandonment) carbon-rich ecosystems. Such an effect has been documented

in previous analyses of scenarios with these economic incentives (Thomson et al. 2011; Wise et al. 2009).

We found that some effects (e.g., global CO_2 emissions, global mean temperature rise) are small at the global scale but larger at the local and regional scale, with significant heterogeneity among regions. At the global level, increases in average productivity lead to declines in total cropland area. At the regional scale, however, the regions with the largest increases in productivity (e.g., parts of Europe and Australia) increase their cropland area, while relatively less-productive regions contract cropland area. Land expansion in response to cropland declines differs across regions, particularly in the RCP8.5.

This research explores several key sensitivities in human—Earth system coupling. However, there are some limitations to our study and many more sensitivities and uncertainties remain. First, we are only including feedbacks on the terrestrial system. Many other human-Earth system feedbacks are possible, including the effects of climate on energy demand (Clarke et al. 2018; Zhou et al. 2014), energy supply (Cronin et al. 2018), water availability (Strzepek et al. 2015; Hejazi et al. 2014; Hanasaki et al. 2013), income (Burke et al. 2015; Woodard et al. 2019), behavior (Beckage et al. 2018), etc. The inclusion of feedbacks in other systems may result in different effects (Calvin and Bond-Lamberty 2018). Additionally, we only pass land use/land cover and energy system CO_2 emissions from GCAM to CESM; we exclude any effects of feedbacks on fertilizer application or resulting N_2O emissions.

Second, we are only using a single climate model (CESM) and IAM when calculating the effect of climate feedbacks. The range of NPP and land cover change across climate models is large, and CESM's relatively weak response of NPP to climate dampens potential feedbacks (Todd-Brown et al. 2013, 2014). Similarly, previous studies have shown a large range in ocean carbon uptake across ESMs, with CESM falling in the middle of that range (Friedlingstein et al. 2014). Additionally, previous studies have shown large differences in land use (Popp et al. 2014, 2017) and emissions (Clarke et al. 2014; Riahi et al. 2017) across IAMs. Thus, choosing a different human or Earth system model could lead to substantially different results.

Third, we are using a single crop model (a linear relationship between NPP and yield) (Bond-Lamberty et al. 2014), but crop models exhibit significant differences in their response of yield to climate (Rosenzweig et al. 2014). Furthermore, the crop model includes the effect of climate and CO_2 on productivity, but excludes the effect of ozone damage which can have significant negative effects on yield (Reilly et al. 2007).

Fourth, while the coupling between the IAM and ESM is in code, we only exchange lagged information every five years, i.e. at the IAM time step (Collins et al. 2015), potentially introducing lag uncertainties (cf. Voldoire et al. (2007)). Future efforts could include simultaneous calculation or a more frequent information exchange.

Finally, previous studies have indicated that some of these feedbacks (e.g., permafrost) are too slow for the timeframes analyzed in this paper (see Schuur et al., 2015). For example, SI Figure 4 shows little effect on ocean carbon uptake due to coupling, suggesting that ocean feedbacks are too slow to be altered by human responses at the timescales in this paper (decades to century). In short, future research is needed to both strengthen the existing linkages between the human and Earth system components of iESM, as well as expand these linkages to capture other feedbacks.

Our research underlines the importance of climate model and emissions scenario uncertainties in climate studies (Hawkins and Sutton 2009; Kirtman et al. 2013), socioeconomics and climate policy in human systems studies (Clarke et al. 2014; Riahi et al. 2017), and the critical nature of uncertainty and sensitivity analyses in future coupled human—Earth system studies. Given the wide range of ESM model results and the inherent difficulties in characterizing models' current and predictive uncertainties (Ricciuto et al. 2008, 2018), there is a need for more coupled human-Earth system models, systematic comparisons between these models, and methods to examine uncertainty and sensitivity in such models. In particular, more coupled human—Earth system models that include dynamic bidirectional interactions between the Earth system and various components of the human system (e.g., water, population, migration, economics, trade, human health) are needed. Additional models and hypothesis testing are needed to determine when and how bidirectional feedbacks between human and Earth systems should be considered in future assessments of climate change.

Acknowledgments

This research was supported as part of the Energy Exascale Earth System Model (E3SM) project, funded by the U.S. Department of Energy, Office of Science, Office of Biological and Environmental Research. This research used resources of the Oak Ridge Leadership Computing Facility, which is a U.S. Department of Energy Office of Science User Facility supported under Contract DE-AC05-00OR22725. This research used resources of the National Energy Research Scientific Computing Center, a DOE Office of Science User Facility supported by the Office of Science of the U.S. Department of Energy under Contract No. DE-AC02-05CH11231. This research also used PNNL Institutional Computing at Pacific Northwest National Laboratory. This work used the Community Earth System Model, CESM and the Global Change Assessment Model, GCAM. The National Science Foundation and the Office of Science of the U.S. Department of Energy support the CESM project. The opinions expressed in this paper are the authors alone.

Data Availability

The iESM model code and input data is available at https://github.com/E3SM-Project/iESM.

All code and most data used in the analysis and figures in this paper are available at: https://github.com/kvcalvin/iesm-45v85. Raw model outputs and large data files (e.g., the data used in Figures 6, 7, and S6), however, are not archived on GitHub due to the size of data. These outputs are available upon request.

References

Anderegg, W. R. L., and Coauthors, 2015: Pervasive drought legacies in forest ecosystems and their implications for carbon cycle models. *Science (80-.).*, **349**, 528–532.

Arent, D. J., R. S. J. Tol, E. Faust, J. P. Hella, S. Kumar, K. M. Strzepek, F. L. Tóth, and D. Yan, 2014: Key economic sectors and services. *Climate Change 2014: Impacts, Adaptation, and Vulnerability. Part A: Global and Sectoral Aspects.*, Cambridge University Press, New York, NY, USA and Cambridge, UK, 659–708.

Arora, V. K., and G. J. Boer, 2014: Terrestrial ecosystems response to future changes in climate and atmospheric CO2 concentration. *Biogeosciences*, **11**, 4157–4171.

Beckage, B., and Coauthors, 2018: Linking models of human behaviour and climate alters projected climate change. *Nat. Clim. Chang.*, **8**, 79–84, doi:10.1038/s41558-017-0031-7. https://doi.org/10.1038/s41558-017-0031-7.

Berndes, G., M. Hoogwijk, and R. van den Broek, 2003: The contribution of biomass in the future global energy supply: a review of 17 studies. *Biomass and Bioenergy*, **25**, 1–28.

Bond-Lamberty, B., and Coauthors, 2014: On linking an Earth system model to the equilibrium carbon representation of an economically optimizing land use model. *Geosci. Model Dev.*, **7**, doi:10.5194/gmd-7-2545-2014.

Brovkin, V., and Coauthors, 2013: Effect of anthropogenic land-use and land-cover changes on climate and land carbon storage in CMIP5 projections for the twenty-first century. *J. Clim.*, **26**, 6859–6881, doi:10.1175/JCLI-D-12-00623.1.

Burke, M., S. M. Hsiang, and E. Miguel, 2015: Global non-linear effect of temperature on economic production. *Nature*, **527**, 235. https://doi.org/10.1038/nature15725.

Calvin, K. V, and B. Bond-Lamberty, 2018: Integrated human-Earth System Modeling -- state of the science and future research directions. *Environ. Res. Lett.*, doi:10.1088/1748-9326/aac642.

Clarke, L., J. Edmonds, H. Jacoby, H. Pitcher, J. Reilly, and R. Richels, 2007: *CCSP Synthesis and Assessment Product 2.1a: Scenarios of Greenhouse Gas Emissions and Atmospheric Concentrations*. U.S. Government Printing Office, Washington D.C.,.

Clarke, L., and Coauthors, 2018: Effects of long-term climate change on global building energy expenditures. *Energy Econ.*, **72**, 667–677, doi:https://doi.org/10.1016/j.eneco.2018.01.003. http://www.sciencedirect.com/science/article/pii/S0140988318300112.

Clarke, L. E., and Coauthors, 2014: Assessing transformation pathways. *Climate Change 2014: Mitigation of Climate Change. Contribution of Working Group III to the Fifth Assessment Report of the Intergovernmental Panel on Climate Change*, 413–510 http://scholar.google.com/scholar?hl=en&btnG=Search&q=intitle:Assessing+Transformation+Pathways#4.

Collins, M., and Coauthors, 2013: Long-term Climate Change: Projections, Commitments and Irreversibility. *Climate Change 2013: The Physical Science Basis. Contribution of Working Group I to the Fifth Assessment Report of the Intergovernmental Panel on Climate Change*, G.-K.P. T. F. Stocker, D. Qin, Ed., Cambridge University Press, Cambridge, United Kingdom and New York, NY, USA.

Collins, W. D., and Coauthors, 2015: The integrated Earth system model version 1: Formulation and functionality. *Geosci. Model Dev.*, **8**, 2203–2219, doi:10.5194/gmd-8-2203-2015.

Cronin, J., G. Anandarajah, and O. Dessens, 2018: Climate change impacts on the energy system: a review of trends and gaps. *Clim. Change*, **151**, 79–93, doi:10.1007/s10584-018-2265-4. https://doi.org/10.1007/s10584-018-2265-4.

Friedlingstein, P., M. Meinshausen, V. K. Arora, C. D. Jones, A. Anav, S. K. Liddicoat, and R. Knutti, 2014: Uncertainties in CMIP5 climate projections due to carbon cycle feedbacks. *J. Clim.*, **27**, 511–526, doi:10.1175/JCLI-D-12-00579.1.

Hallegatte, S., and K. J. Mach, 2016: Make climate-change assessments more relevant. *Nature*, **534**, 613–615.

Hallgren, W., C. A. Schlosser, E. Monier, D. Kicklighter, A. Sokolov, and J. Melillo, 2013: Climate impacts of a large-scale biofuels expansion. *Geophys. Res. Lett.*, doi:10.1002/grl.50352.

Hanasaki, N., and Coauthors, 2013: A global water scarcity assessment under Shared Socio-economic Pathways - Part 2: Water availability and scarcity. *Hydrol. Earth Syst. Sci.*, **17**, 2393–2413, doi:10.5194/hess-17-2393-2013.

Hawkins, E., and R. Sutton, 2009: The Potential to Narrow Uncertainty in Regional Climate Predictions. *Bull. Am. Meteorol. Soc.*, **90**, 1095–1107.

Hejazi, M. I., and Coauthors, 2014: Integrated assessment of global water scarcity over the 21st century under multiple climate change mitigation policies. *Hydrol. Earth Syst. Sci.*, **18**, 2859–2883, doi:10.5194/hess-18-2859-2014.

Holm, J. A., J. Q. Chambers, W. D. Collins, and N. Higuchi, 2014: Forest response to increased disturbance in the central Amazon and comparison to western Amazonian forests. *Biogeosciences*, **11**, 5773–5794.

Houghton, R. A., J. I. House, J. Pongratz, G. R. van der Werf, R. S. DeFries, M. C. Hansen, C. Le Quéré, and N. Ramankutty, 2012: Carbon emissions from land use and land-cover change. *Biogeosciences*, **9**, 5125–5142.

Hurrell, J. W., and Coauthors, 2013: The Community Earth System Model: A Framework for Collaborative Research. *Bull. Am. Meteorol. Soc.*, **94**, 1339–1360.

Jones, A. D., and Coauthors, 2013: Greenhouse gas policy influences climate via direct effects of land-use change. *J. Clim.*, **26**, 3657–3670, doi:10.1175/JCLI-D-12-00377.1.

Kirtman, B., and Coauthors, 2013: Near-term Climate Change: Projections and Predictability. *Climate Change 2013: The Physical Science Basis. Contribution of Working Group I to the Fifth Assessment Report of the Intergovernmental Panel on Climate Change*, T. Stocker, D. Qin, and G.-K. Plattner, Eds., Cambridge University Press, Cambridge, United Kingdom and New York, NY, USA.

Long, M. C., K. Lindsay, S. Peacock, J. K. Moore, and S. C. Doney, 2013: Twentieth-Century Oceanic Carbon Uptake and Storage in CESM1(BGC). *J. Clim.*, **26**, 6775–6800, doi:10.1175/JCLI-D-12-00184.1. https://doi.org/10.1175/JCLI-D-12-00184.1.

Moss, R. H., and Coauthors, 2010: The next generation of scenarios for climate change research and assessment. *Nature*, **463**, 747.

Motesharrei, S., and Coauthors, 2016: Modeling sustainability: population, inequality, consumption, and bidirectional coupling of the Earth and Human Systems. *Natl. Sci. Rev.*, **3**, 470–494. http://dx.doi.org/10.1093/nsr/nww081.

Nelson, G. C., and Coauthors, 2014: Climate change effects on agriculture: Economic responses to biophysical shocks. *Proc. Natl. Acad. Sci.*, **111**, 3274–3279, doi:10.1073/pnas.1222465110. http://www.pnas.org/lookup/doi/10.1073/pnas.1222465110.

Palmer, P. I., and M. J. Smith, 2014: Model human adaptation to climate change. *Nature*, **512**, 365–366, doi:10.1038/512365a.

Piao, S., P. Ciais, P. Friedlingstein, N. de Noblet-Ducoudré, P. Cadule, N. Viovy, and T. Wang, 2009: Spatiotemporal patterns of terrestrial carbon cycle during the 20th century. *Global Biogeochem. Cycles*, **23**.

Popp, A., and Coauthors, 2014: Land-use transition for bioenergy and climate stabilization: Model comparison of drivers, impacts and interactions with other land use based mitigation options. *Clim. Change*, **123**, 495–509,

doi:10.1007/s10584-013-0926-x.

——, and Coauthors, 2017: Land-use futures in the shared socio-economic pathways. *Glob. Environ. Chang.*, **42**, 331–345, doi:10.1016/j.gloenvcha.2016.10.002. http://dx.doi.org/10.1016/j.gloenvcha.2016.10.002.

Reilly, J., and Coauthors, 2007: Global economic effects of changes in crops, pasture, and forests due to changing climate, carbon dioxide, and ozone. *Energy Policy*, **35**, 5370–5383, doi:10.1016/j.enpol.2006.01.040.

Riahi, K., and Coauthors, 2011: RCP 8.5-A scenario of comparatively high greenhouse gas emissions. *Clim. Change*, **109**, 33–57, doi:10.1007/s10584-011-0149-y.

Riahi, K., and Coauthors, 2017: The Shared Socioeconomic Pathways and their energy, land use, and greenhouse gas emissions implications: An overview. *Glob. Environ. Chang.*, **42**, doi:10.1016/j.gloenvcha.2016.05.009.

Ricciuto, D., K. Sargsyan, and P. Thornton, 2018: The Impact of Parametric Uncertainties on Biogeochemistry in the E3SM Land Model. *J. Adv. Model. Earth Syst.*, **10**.

Ricciuto, D. M., K. J. Davis, and K. Keller, 2008: A Bayesian calibration of a simple carbon cycle model: The role of observations in estimating and reducing uncertainty. *Global Biogeochem. Cycles*, **22**.

Rosenzweig, C., and Coauthors, 2014: Assessing agricultural risks of climate change in the 21st century in a global gridded crop model intercomparison. *Proc. Natl. Acad. Sci.*, **111**, 3268–3273, doi:10.1073/pnas.1222463110. http://www.pnas.org/lookup/doi/10.1073/pnas.1222463110.

Shao, P., X. Zeng, K. Sakaguchi, R. K. Monson, and X. Zeng, 2013: Terrestrial Carbon Cycle: Climate Relations in Eight CMIP5 Earth System Models. *J. Clim.*, **26**, 8744–8764.

Strzepek, K., and Coauthors, 2015: Benefits of greenhouse gas mitigation on the supply, management, and use of water resources in the United States. *Clim. Change*, **131**, doi:10.1007/s10584-014-1279-9.

Thomson, A. M., and Coauthors, 2011: RCP4.5: A pathway for stabilization of radiative forcing by 2100. *Clim. Change*, **109**, doi:10.1007/s10584-011-0151-4.

Thornton, P. E., and Coauthors, 2009: Carbon-nitrogen interactions regulate climate-carbon cycle feedbacks: results from an atmosphere-ocean general circulation model. *Biogeosciences*, **6**, 2099–2120, doi:10.5194/bg-6-2099-2009. https://www.biogeosciences.net/6/2099/2009/.

Thornton, P. E. P. E., and Coauthors, 2017: Biospheric feedback effects in a

synchronously coupled model of human and Earth systems. *Nat. Clim. Chang.*, **7**, 496–500, doi:10.1038/nclimate3310.

Todd-Brown, K. E. O., J. T. Randerson, W. M. Post, F. M. Hoffman, C. Tarnocai, E. A. G. Schuur, and S. D. Allison, 2013: Causes of variation in soil carbon simulations from CMIP5 Earth system models and comparison with observations. *Biogeosciences*, **10**, 1717–1736.

——, and Coauthors, 2014: Changes in soil organic carbon storage predicted by Earth system models during the 21st century. *Biogeosciences*, **11**, 2341–2356.

Voldoire, A., B. Eickhout, M. Schaeffer, J. F. Royer, and F. Chauvin, 2007: Climate simulation of the twenty-first century with interactive land-use changes. *Clim. Dyn.*, **29**, 177–193, doi:10.1007/s00382-007-0228-y.

van Vuuren, D. P., and Coauthors, 2011: The representative concentration pathways: An overview. *Clim. Change*, **109**, 5–31, doi:10.1007/s10584-011-0148-z.

Wise, M., and Coauthors, 2009: Implications of Limiting CO2 Concentrations for Land Use and Energy. *Science (80-.).*, **324**, 1183–1186, doi:10.1038/ncb2099.

——, K. Calvin, P. Kyle, P. Luckow, and J. Edmonds, 2014: Economic and Physical Modeling of Land Use in Gcam 3.0 and an Application To Agricultural Productivity, Land, and Terrestrial Carbon. *Clim. Chang. Econ.*, **05**, 1450003, doi:10.1142/S2010007814500031. http://www.worldscientific.com/doi/abs/10.1142/S2010007814500031.

Woodard, D. L., S. J. Davis, and J. T. Randerson, 2019: Economic carbon cycle feedbacks may offset additional warming from natural feedbacks. *Proc. Natl. Acad. Sci.*, **116**, 759 LP-764, doi:10.1073/pnas.1805187115. http://www.pnas.org/content/116/3/759.abstract.

Yang, S., W. Dong, J. Chou, J. Feng, and X. Yan, 2015: A Brief Introduction to BNU-HESM1 . 0 and Its Earth Surface Temperature Simulations. **32**, 1683–1688, doi:10.1007/s00376-015-5050-6.1.

Zhou, Y., and Coauthors, 2014: Modeling the effect of climate change on U . S . state-level buildings energy demands in an integrated assessment framework. *Appl. Energy*, **113**, 1077–1088, doi:10.1016/j.apenergy.2013.08.034. http://dx.doi.org/10.1016/j.apenergy.2013.08.034.